High Vp/Vs ratio: Saturated cracks or anisotropy effects?

X.-Q. Wang,[1,2] A. Schubnel,[2] J. Fortin,[2] E. C. David,[3] Y. Guéguen,[2] and H.-K. Ge[4]

Received 19 March 2012; revised 10 May 2012; accepted 14 May 2012; published 8 June 2012.

[1] We measured Vp/Vs ratios of thermally cracked Westerly granite, thermally cracked Carrara marble and 4% porosity Fontainebleau sandstone, for an effective mean pressure ranging from 2 to 95 MPa. Samples were fluid-saturated alternatively with argon gas and water (5 MPa constant pore pressure). The experimental results show that at ultrasonic frequencies, Vp/Vs ratio of water saturated specimen never exceeded 2.15, even at effective mean pressure as low as 2 MPa, or for a lithology for which the Poisson's ratio of minerals is as high as 0.3 (calcite). In order to check these results against theoretical models: we examine first a randomly oriented cracked medium (with dispersion but without anisotropy); and second a medium with horizontally aligned cracks (with anisotropy but without dispersion). The numerical results show that experimental data agree well with the first model: at high frequency, Vp/Vs ratios range from 1.6 to 1.8 in the dry case and from 1.6 to 2.2 in the saturated case. The second model predicts both Vp/Sv and Vp/Sh to vary from 1.2 to 3.5, depending on the raypath angle relative to the crack fabric. In addition, perpendicular to the crack fabric, a high Vp/Vs ratio is predicted in the absence of shear wave splitting. From these results, we argue the possibility that high Vp/Vs ratio (>2.2) as recently imaged by seismic tomography in subduction zones, may come from zones presenting important crack anisotropy. The cumulative effects of crack anisotropy and high pore fluid pressure are required to get Vp/Vs ratios above 2.2. **Citation:** Wang, X.-Q., A. Schubnel, J. Fortin, E. C. David, Y. Guéguen, and H.-K. Ge (2012), High Vp/Vs ratio: Saturated cracks or anisotropy effects?, *Geophys. Res. Lett.*, *39*, L11307, doi:10.1029/2012GL051742.

1. Introduction

[2] Vp/Vs ratio is an important rock diagnostic parameter, which can be directly determined by seismology. Indeed, recent tomographic studies [*Kodaira et al.*, 2004; *Audet et al.*, 2009] performed on the Japanese and Cascadian subduction zones have emphasized the existence of a thin layer of high Vp/Vs ratio (>2.1). Based on ultrasonic measurements (>50 kHz) performed in the laboratory on crystalline rocks under water saturated conditions [*Christensen*, 1984; *Peacock et al.*, 2011], these high Vp/Vs zones have often been interpreted as regions of high pore fluid pressure [*Kodaira et al.*, 2004; *Audet et al.*, 2009; *Peacock et al.*, 2011]. An alternative hypothesis is that of *Mainprice and Ildefonse* [2009] and *Bezacier et al.* [2010], who propose that regions of high Vp/Vs ratios and low velocities may be due to strong mineral preferred orientation, serpentine in particular.

[3] In an isotropic rock, Vp/Vs ratio directly reflects the variation of Poisson's ratio, $\upsilon = 0.5(1 - 1/[(Vp/Vs)^2 - 1])$. In an anisotropic medium however, the Poisson's ratio is not unique and will depend on the orientation of the wave propagation [*Mavko et al.*, 1998]. In cracked rocks for instance, crack density and geometry influence elastic wave velocity [*Walsh*, 1965] while crack fabric (preferential orientation) may result in the development of elastic anisotropy [*Nishizawa*, 1982]. When rocks are fluid saturated, the frequency dispersion of P and S wave velocities between laboratory (ultrasonic, >kHz) and seismic (<10 Hz) frequencies should also be considered [*Murphy*, 1985; *Winkler*, 1986,]. In this study, we measure and compare the Vp/Vs ratio obtained on three standards of Rock Physics (Westerly granite, Carrara marble and Fontainebleau sandstone) as a function of effective mean pressure.

[4] In order to check these experimental results against theoretical models, using Effective Medium Theory (EMT) as a tool, we then examine two different models. The first one consists of a randomly oriented cracked medium (with dispersion but without anisotropy), similar to the first two experiments. The second one consists of horizontally aligned cracks (with anisotropy but without dispersion). Using these models, the high frequency (MHz-laboratory case, HF for abbreviation) effective elastic properties can be completely calculated as functions of the crack density and crack geometry. Low frequency (kHz-field and below, LF for abbreviation) moduli are calculated from the Biot-Gassmann [*Biot*, 1956] and *Brown and Korringa* [1975] equations. From these moduli, we investigate how the crack density, geometry and the crack orientation influence the "apparent" Vp/Vs ratio at high and low frequencies.

2. Experimental Results

[5] The materials used in our experiments are natural Westerly granite, Carrara marble and Fontainebleau sandstone. All experiments were conducted under hydrostatic stress on a triaxial cell installed in the Laboratoire de Géologie at Ecole Normale Supérieure. A complete description of the experimental set-up is given in *Brantut et al.* [2012] and *Ougier-Simonin et al.* [2011]. Samples were cored and polished as cylinders of 80 mm length and 40 mm diameter. Vp and Vs elastic velocities were measured along diameters

[1]Key Laboratory of Seismic Observation and Geophysical Imaging, Institute of Geophysics, CEA, Beijing, China.
[2]Laboratoire de Géologie, UMR 8538, Ecole Normale Supérieure, CNRS, Paris, France.
[3]Department of Earth Science and Engineering, Imperial College, London, UK.
[4]Unconventional Natural Gas Institute, China University of Petroleum, Beijing, China.

Corresponding author: X.-Q. Wang, Laboratoire de Géologie, UMR 8538, Ecole Normale Supérieure, CNRS, 24 Rue Lhomond, F-75005 Paris CEDEX, France. (wxq4526@gmail.com)

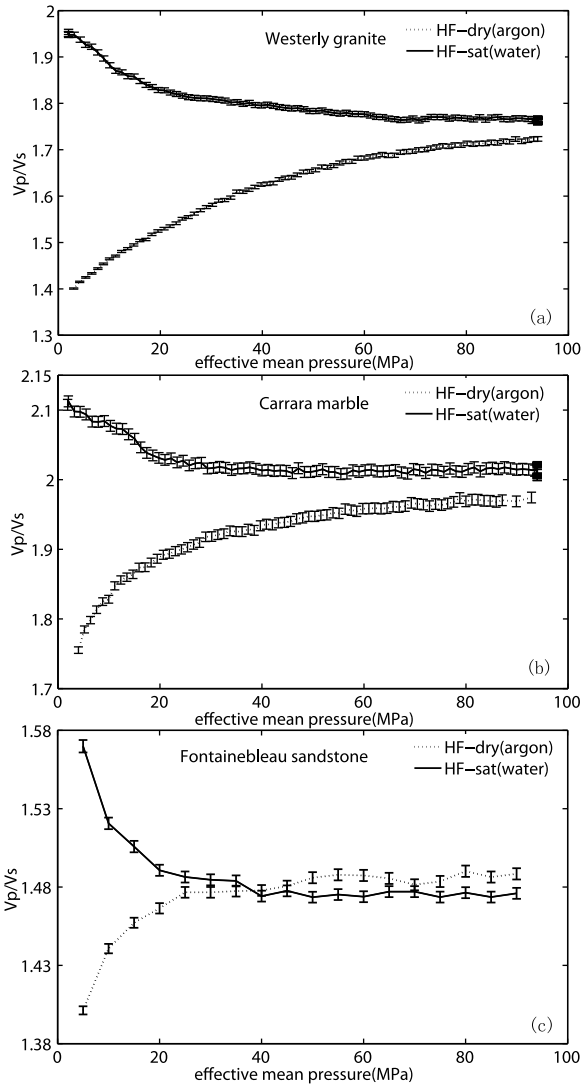

Figure 1. Ultrasonic measurements of Vp/Vs ratio evolution as a function of effective mean pressure of (a) thermally cracked Westerly granite; (b) thermally cracked Carrara marble; (c) 4% porosity Fontainebleau sandstone. The dotted lines indicate measurements performed under argon saturation. The solid lines indicate water saturation case. Error bar has been also shown. Note that these three plots have different vertical scales.

of the samples, under hydrostatic condition, for an effective mean pressure ranging from 2 to 95 MPa. Samples were fluid-saturated alternatively with argon gas and water (5 MPa constant pore pressure). The relative error on velocity measurements is estimated to be lower than 1%.

[6] Figure 1 presents experimental measurements of Vp/Vs ratios on three standards: a) Westerly granite, b) Carrara marble, c) Fontainebleau sandstone. The modal composition and elastic moduli are given in Table 1. The marble and granite samples were initially thermally shocked at 700°C, in order to create a homogeneous and randomly oriented crack-like porosity of about 1%. The Fontainebleau sandstone presents an initial porosity of equant-like pores of approximately 4% [*David*, 2012]. Our experimental results show that, saturated with a compressible fluid such as argon, Vp/Vs ratio increases with increasing effective pressure in all three specimens. When saturated with an incompressible fluid such as water, however, it decreases with increasing effective pressure in all three specimens. If we interpret the curves of Figure 1 as a result of crack closure process, this implies a closure pressure of about 100 MPa in the case of the two thermally shocked samples (Westerly granite and Carrara marble) and 30 MPa for the Fontainebleau sandstone. As expected, the cracks effect is much smaller in the case of Fontainebleau sandstone, which was not thermally shocked. Moreover, as the non-closable porosity of this rock is small, the lower Vp/Vs ratios observed in this case (about 1.5) are simply explained by the small value of Poisson's ratio of the pure quartz grains [*Fortin et al.*, 2007; *David*, 2012]. This observation highlights that in water saturated specimen, the shape of pores plays a major role on Vp/Vs ratio. In all three cases, Vp/Vs ratio of water saturated specimen never exceeded 2.15, even at effective mean pressures as low as 2 MPa, or for a lithology for which the Poisson's ratio of the minerals is as high as 0.3 (calcite). At low effective mean pressure, the high frequency Vp/Vs ratio of water-saturated condition is much larger than that of the dry case, because of both the crack and fluid effects. However, both such effects decrease when the effective mean pressure increases, as the cracks close gradually. In addition, the Vp and Vs evolution versus effective mean pressure are also shown in the auxiliary material.[1]

3. Theoretical Background

[7] Comparing laboratory data to seismic observations and to predicted values is possible using crack models. According to the non-interactive approximation (NIA), an elastic solid containing many cracks can be treated as the sum of individual sources of extra strains (since cracks are more compliant than the matrix) due to each singular crack. Thus for planar cracks of circular shape, the extra compliance due to cracks can be calculated. The detailed information has been given in *Kachanov* [1993] and *Guéguen and Sarout* [2009]. As a seismic wave passes through a fluid saturated rock sample, the dispersion of P- and S- waves between seismic frequencies (LF) and laboratory frequencies (HF) should not be ignored [*Biot*, 1956; *Murphy*, 1985; *Dvorkin et al.*, 1995; *Le Ravalec and Guéguen*, 1996;

[1]Auxiliary materials are available in the HTML. doi:10.1029/2012GL051742.

Table 1. Modal Composition and Initial Matrix Elastic Moduli of the Three Tested Rock Samples

	Composition	Young Modulus and Initial Poisson Ratio	Initial Porosity
Westerly Granite	27% quartz, 36% microcline, 30% plagioclase, 6% biotite	E0 = 80 GPa, υ_0 = 0.25	1.7% (thermally)
Carrara Marble	>99% calcite	E0 = 93 GPa, υ_0 = 0.34	0.6% (thermally)
Fontainebleau Sandstone	>99% quartz	E0 = 94 GPa, υ_0 = 0.08	4%

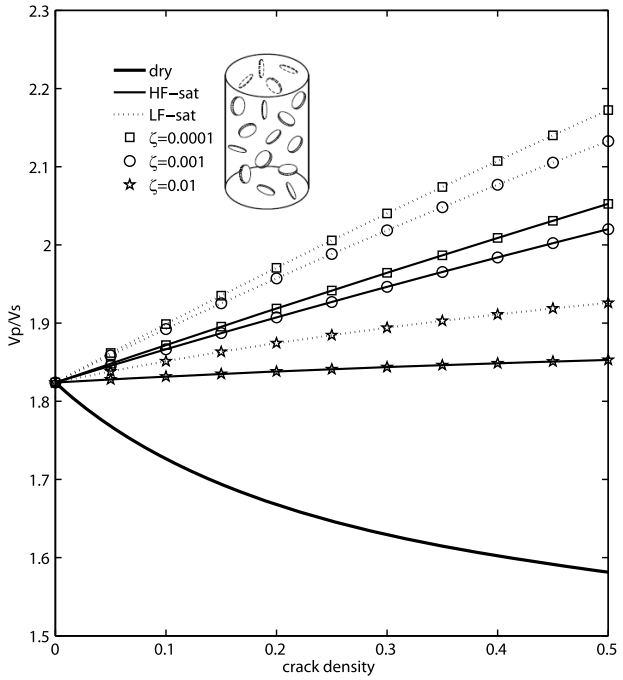

Figure 2. Vp/Vs ratio at LF (dotted line) and HF (solid line) plotted versus crack density (range from 0 to 0.5) for a randomly cracked isotropic medium. Curves are given for fixed aspect ratio ζ of 10^{-4} (squares), 10^{-3} (circles) and 10^{-2} (stars). The dry case is plotted as a reference (bold solid curve).

Adelinet et al., 2010]. While high frequency elastic compliances can be obtained from NIA theory, the low frequency compliances can be obtained from Biot's theory. *Brown and Korringa* [1975] have extended the Biot-Gassmann equations to express the undrained compliances (low frequency moduli) in terms of the dry ones in a Tranversely Isotropic (TI) medium. Following *Guéguen and Sarout* [2009], the difference between HF and LF wave velocities depends only on the crack density tensors, the solid matrix elastic parameters, the fluid bulk modulus and the crack aspect ratio. HF and LF elastic moduli can be inverted from the compliances, in such a way that the dispersion due to local fluid flow mechanisms can be defined by the difference of HF and LF elastic parameters [*Adelinet et al.*, 2010]. In terms of these compliance constants, the three phase velocities Vp, Vsv and Vsh can then be written conveniently as a function of the angle θ between the TI symmetry axis and the propagation direction [*Mavko et al.*, 1998].

[8] *Thomsen* [1986] introduced three dimensionless parameters, γ, δ, ϵ, which characterize the extent of anisotropy. In a transversely isotropic (TI) medium, these three parameters, together with the velocities $V_P^0 = \sqrt{c_{33}/\rho}$ and $V_S^0 = \sqrt{c_{44}/\rho}$, where ρ is the rock bulk density, fully characterize the rock elastic properties [*Mavko et al.*, 1998]. In the following model, we will use Thomsen's parameters to characterize the anisotropy of TI medium.

4. Numerical Results

[9] In all the modeling below, we use the same reference values for the crack-free matrix elastic constants, i.e., a Young's modulus and Poisson's ratio of $E_0 = 80.5$ GPa and $\nu_o = 0.28$ respectively, close to granite values (Table 1). The pore fluid (water) bulk modulus is taken as $K_f = 2.3$ GPa. Solid and fluid densities are respectively $\rho_s = 2700$ kg m^{-3} and $\rho_f = 1000$ kg m^{-3}.

4.1. Isotropic Case: Effects of Frequency on Vp/Vs

[10] Randomly oriented cracks distribution obviously results in zero anisotropy. This case typically corresponds to the case of thermal cracking as observed experimentally above (Figure 1). Here, we only investigate the effects of crack density, crack aspect ratio and frequency on Vp/Vs. For random crack distributions, the crack density tensor is a scalar. According to NIA, we calculate the HF wet and dry moduli. LF moduli are calculated using the Biot-Gassmann equations. Figure 2 displays Vp/Vs ratio as a function of crack density and crack aspect ratios ζ at HF (solid line) and LF (dotted line). The dry case is also given. We allow the crack density to vary from 0 to 0.5 and the crack aspect ratio from 10^{-4} to 10^{-2}. The limit range of validity of the NIA approximation for penny-shaped cracks is close to ($0 \sim 0.2$) [*Kachanov*, 1993; *Saenger et al.*, 2004]. This is also the range of crack densities and crack aspect ratios found in crystalline rocks [*Schubnel et al.*, 2006; *Fortin et al.*, 2011]. After the Biot-Gassmann correction, Vp/Vs ratio at LF is found to be a little higher than at HF, and there is only a limited fluid dispersion effect. On the contrary, for crack aspect ratios smaller than 10^{-2}, Vp/Vs ratio increases with increasing crack density. In the case of extremely thin cracks (10^{-3}–10^{-4}), and at high frequency, Vp/Vs can reach values larger than 2 for crack densities larger than 0.4. This is in good agreement with experimental data obtained on both thermally cracked Westerly granite and Carrara marble (Figures 1a and 1b). However, in this case, the Biot-Gassmann correction becomes non-neglible because fluid dispersion increases with decreasing ζ. Here, there is no bulk modulus dispersion, but only shear modulus dispersion. Because both Vp and Vs depend on the shear modulus, Vp/Vs ratio dispersion is observed. However, Vs obviously has larger fluid dispersion than Vp, which is why LF Vp/Vs ratio is higher than HF Vp/Vs ratio. At LF, a maximum Vp/Vs ratio of 2.1∼2.2 is obtained for rocks with crack densities of 0.5 and for aspect ratio ζ smaller than 10^{-2}. This shows that fluid effects are mainly important for low aspect ratio, compliant cracks. From Figure 2, we can see that the predicted values at ζ of 10^{-4} and 10^{-3} are very close, so that in the following, we will only consider ζ of 10^{-4} and 10^{-2}.

4.2. Anisotropic Case: Effect of Raypath Direction on "Apparent" Vp/Vs Ratio

[11] We consider horizontally aligned cracks, which results in maximum anisotropy. We have no experimental data for that case, however the good agreement between experimental data and theoretical prediction in the isotropic case is a good reason to explore theoretically the anisotropic case. In this case, all cracks are identical in shapes and orientation. The cracks normals are parallel to the vertical axis. Cracks are subjected to the same boundary condition, so that the fluid pressure in each crack is equal. Therefore the pore fluid is isobaric, even at high frequency, suppressing the possibility of local fluid flow. There is thus no fluid-flow induced dispersion. Hence, we will only consider the effect of anisotropy on Vp/Vs ratio variation. In this particular

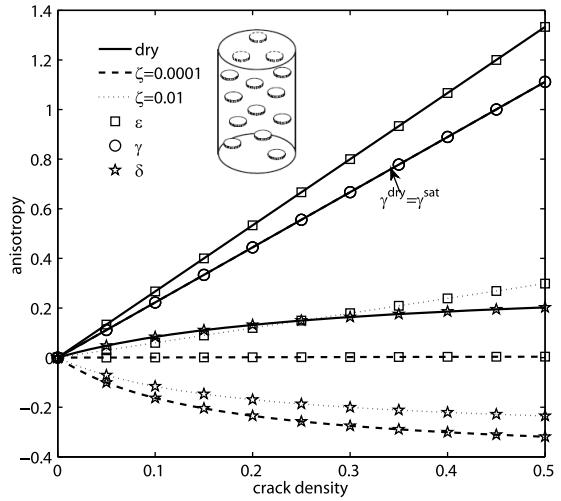

Figure 3. Thomsen's anisotropy parameters (γ, δ, ε) as a function of crack density in a dry and a water saturated anisotropic medium. Square symbols correspond to ϵ, circles to γ and stars to δ. The bold solid line corresponds to the dry case, while the dashed line and grey dotted line correspond to the saturated case with crack aspect ratio of 10^{-4} and 10^{-2} respectively.

case, the crack density tensors have a single non-zero component. Using NIA and Thomsen's formulation to characterize the anisotropy, Figure 3 displays the anisotropy parameters (γ, ε, δ) as a function of crack density and crack aspect ratio in dry and saturated conditions. According to the phase velocities, we can get $\epsilon = (V_P(90) - V_P(0))/V_P(0)$ and $\gamma = (V_{Sh} - V_{Sv})/V_{Sv}$, so that ϵ measures P wave anisotropy and γ measures shear wave anisotropy (shear wave splitting). For reference, three solid lines indicate the dry case. For fluid-saturated cracks, the dashed lines correspond to crack aspect ratio ζ of 10^{-4}, while the dotted lines to crack aspect ratio ζ of 10^{-2}.

[12] Figure 3 highlights that lower aspect ratio ζ values and higher crack density induce larger P wave and shear wave anisotropy. In the saturated case however, ε can be negligible even at large crack density, as long as the crack aspect ratio ζ is smaller than 10^{-2}. This shows that fluid saturation effects on P wave anisotropy are mainly important for low crack aspect ratio and high crack density. As a result of poroelasticity assumptions, γ is insensitive to the presence of fluid (i.e., identical in the dry and in the saturated cases). In both cases, γ increases with crack density, so that shear wave splitting cannot be ignored and both Vp/Sv and Vp/Sh ratio need to be considered independently, as a function of the propagation angle varying from 0° to 90°. Because of $\Delta(V_p/V_s)/(V_p/Vs) = \varepsilon - \gamma$, Figure 3 shows that Vp/Vs can vary by as much as 100% due to saturation.

[13] Figure 4 displays Vp/Sv and Vp/Sh ratios evolution as a function of the raypath angle relative to the crack fabric (varying from 0°, perpendicular to the crack fabric, to 90°, parallel to the crack fabric). Curves are plotted against crack densities of 0.1 (squares), 0.25 (circles) and 0.5 (stars). Solid lines correspond to the dry case, dashed lines to saturated cracks with an aspect ratio of 10^{-4}, dotted lines to saturated cracks with an aspect ratio of 10^{-2}. Figure 4 demonstrates that both the "apparent" Vp/Sv and Vp/Sh ratios can vary, from 1.2 to 3.5, depending on the propagation direction, the crack density and crack aspect ratio. Maximum "apparent" Vp/Vs ratios (>2.5) are obtained for crack densities larger than 0.25 and low aspect ratios ($<10^{-2}$), for wave propagating perpendicular to the crack fabric (for both Sv and Sh waves) or along to the crack fabric (for Sv waves only). Two interesting observations can be made: i) for waves propagating parallel to crack plane, Vp/Vsv can be large irrespective of the crack aspect ratio or the saturation conditions; ii) for waves propagating perpendicular to the crack fabric, Sv and Sh show no difference (i.e., no shear wave splitting) and high "apparent" Vp/Vs ratios will nevertheless be observed for thin cracks (low aspect ratios) saturated with fluids for both shear wave polarizations. We conclude from these theoretical considerations that crack induced elastic anisotropy can have a major influence on the "apparent" Vp/Vs ratio.

5. Discussion

[14] A first point is that our experimental results show that maximum Vp/Vs values at HF in the laboratory are obtained at low effective mean pressure (i.e., high pore fluid pressure), in pervasively isotropic microcracked specimen saturated

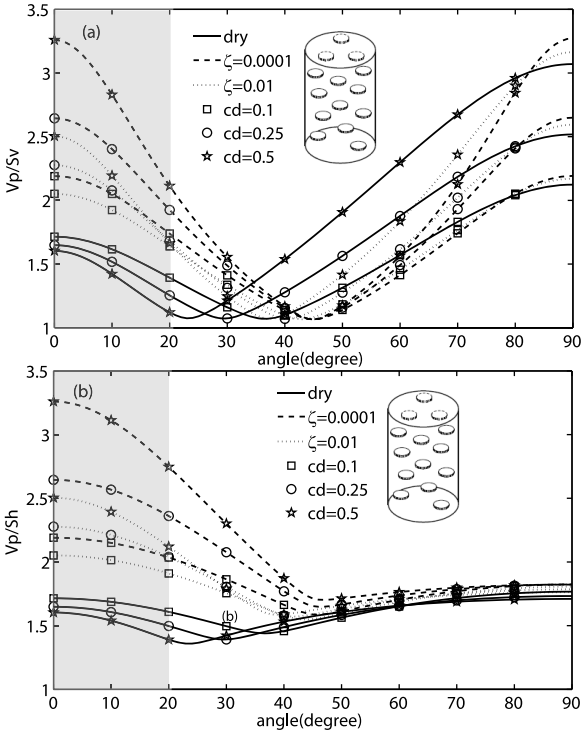

Figure 4. (a) Vp/Sv and (b) Vp/Sh evolutions as a function of wave propagation direction (0° perpendicular to the crack fabric, 90° parallel to the crack fabric) in a dry and water saturated anisotropic cracked rock. "cd" denotes the crack density ranging from 0.1 to 0.5. Square, circle and pentagon symbols represent different crack density respectively. The solid line corresponds to the dry case, while the dashed and dotted lines to the saturated case with constant crack aspect ratio10^{-4} and 10^{-2} respectively. The shaded area represents the typical dip angle of high Vp/Vs layers observed in the Japanese and Cascadian subduction zones at depth ranging between 30 and 60 km [*Kodaira et al.*, 2004; *Audet et al.*, 2009].

with water. Vp/Vs can reach values of 2.15 if the cracks are numerous, thin (aspect ratios lower than 10^{-2}) and saturated with an incompressible fluid such as water. These results are consistent with former laboratory studies [*Christensen*, 1984; *Peacock et al.*, 2011]. Once corrected using the Biot-Gassmann equation, we show that under such conditions (pervasive low aspect ratios microcracks saturated with incompressible fluid), Vp/Vs values could remain high and close to 2.2, even at seismic frequencies. In such a way, the modern interpretation of high Vp/Vs ratios corresponding to high pore fluid pressure [*Kodaira et al.*, 2004; *Audet et al.*, 2009] is a valid hypothesis. With effective mean pressure increasing however, the cracks would gradually close, so that high pore fluid pressures would have to be maintained and ubiquitous in the Vp/Vs anomalous zones. Note that for an aspect ratio $\zeta = 10^{-3}$ and a Young modulus E = 80 GPa, the crack closure pressure is $P_{ce} \approx \zeta E \approx 80$ MPa. The implication is that cracks can remain open only if the effective pressure [i.e., $(P\text{-}P_{fluid})$] is low. Using crack micromechanics, we have shown theoretically that the "fluid microcracked" based interpretation is limited to Vp/Vs ratio values of 2.2–2.3, because realistically, in the pressure conditions at these depths, crack densities cannot reach values much larger than 0.5, and probably are lower. Hence, such hypothesis would fail at least at explaining field scale observations made by *Audet et al.* [2009] of Vp/Vs ratios up to 2.35 (and up to 2.8 in certain areas).

[15] A second important point is that for relatively moderate crack densities, irrespective to the presence of fluids, crack induced elastic anisotropy can create large "apparent" variations of Vp/Vsv and Vp/Vsh (from 1.2 to 3.5 – see Figure 4), both perpendicular and parallel to the crack fabric. Importantly, perpendicular to the crack fabric, high "apparent" Vp/Vs ratio can be observed in the absence of shear wave splitting. This has been shown using again theoretical crack micromechanics. Unfortunately, laboratory measurements of crack induced elastic wave anisotropy at ultrasonic frequencies in initially isotropic crystalline rocks are scarce [*Schubnel et al.*, 2006; *Stanchits et al.*, 2006]. Although the symmetry is often that of radial cracks, due to experimental limitations, the experimental results nevertheless confirm the theoretical observations presented in this paper. Ultrasonic measurements on rocks containing anisotropic fabrics, both mineral and crack induced, are more common however. For example, *Nishizawa and Kanagawa* [2010] have recently observed "apparent" Vp/Vs ratio as high as 2.4, for waves propagating parallel to the crack and mineral fabrics in biotite rich micaschists, under dry and elevated pressure (150 MPa) conditions. Similarly, *Sarout and Guéguen* [2008] observed Vp/Vsv ratios of 2.35 in dry consolidated clays for wave propagating parallel to the fabric, under 200 MPa isotropic stress.

[16] Further work is needed to go beyond our present understanding and several questions remain open. It is often argued that the source of pore fluid pressure at depth comes from mineral dehydration, in particular serpentine. However, *Popp and Kern* [1993] showed that Vp/Vs ratio decreased during serpentine dehydration under high hydrostatic stress, because mineral dehydration also generally involves replacing a soft phase by a stiffer one. More recently, *Brantut et al.* [2012] made the same observations during gypsum dehydration in hydrostatic and drained conditions, for two different (and moderate) effective pressures (10 and 55 MPa). Importantly, they also showed that mineral dehydration, under non-hydrostatic stress, was accompanied by dehydration-induced crack anisotropy, probably linked to the preferential opening of mineral cleavage planes parallel to the maximum compressive stress.

6. Conclusion

[17] Finally, the shaded area on Figure 4 highlights the typical dip angle of high Vp/Vs layers found in the Cascadian [*Audet et al.*, 2009] and Japanese subduction zones [*Kodaira et al.*, 2004]. Assuming a crack fabric more or less parallel to the layer (or the slab dip), receiver functions methods, because they use teleseismic rays, would sample raypaths more or less perpendicular to the crack fabric. This is precisely the case for which one could observe a high apparent Vp/Vs ratio, and yet no shear wave splitting (Figure 4). From the above analysis, we conclude that the possible influence of crack-induced anisotropy on "apparent" Vp/Vs ratio cannot be simply eluded in subduction zone environments, especially when field geology systematically points out that rocks, which went down the subduction channel and were then brought back to the surface, almost systematically present important mineral and crack fabrics (foliations). From which we argue the possibility that high Vp/Vs ratio (>2.2) as recently imaged by seismic tomography in subduction zones, may come from zones presenting important crack anisotropy and/or mineral fabric, as argued by *Bezacier et al.* [2010]. Such hypothesis does not exclude the role played by incompressible fluid saturation. Indeed, we showed that, for waves propagating perpendicular to the crack fabric, apparent high Vp/Vs values can only be found for low aspect ratio saturated microcrack fabrics. This means at such depth that, there is a high pore pressure to keep the cracks open. The source of fluids and crack fabric could correspond to dehydrating rocks under non-hydrostatic stress. The implication is that high Vp/Vs ratio would be the result of high pore fluid pressure and crack anisotropy, the second effect amplifying the first one.

[18] **Acknowledgments.** This work was funded by Institut National des Sciences de l'Univers (programme Faille Fluide Flux) and by the NSFC (National Natural Science Foundation of China, grant 41174040). The authors would like to acknowledge the technical help of Yves Pinquier. The authors thank the reviewers for their useful comments.

[19] The Editor thanks Erik Saenger and an anonymous reviewer for assisting in the evaluation of this paper.

References

Adelinet, M., J. Fortin, Y. Guéguen, A. Schubnel, and L. Geoffroy (2010), Frequency and fluid effects on elastic properties of basalt: Experimental investigations, *Geophys. Res. Lett.*, *37*, L02303, doi:10.1029/2009GL041660.

Audet, P., M. G. Bostock, N. I. Christensen, and S. M. Peacock (2009), Seismic evidence for overpressured subducted oceanic crust and megathrust fault sealing, *Nature*, *457*, 76–78, doi:10.1038/nature07650.

Bezacier, L., B. Reynard, J. D. Bass, C. Sanchez-Valle, and B. V. Moortele (2010), Elasticity of antigorite, seismic detection of serpentinites, and anisotropy in subduction zones, *Earth Planet. Sci. Lett.*, *289*, 198–208, doi:10.1016/j.epsl.2009.11.009.

Biot, M. (1956), Theory of propagation of elastic waves in a fluid saturated porous solid. I. Low-frequency range, *J. Acoust. Soc. Am.*, *28*(2), 168–178, doi:10.1121/1.1908239.

Brantut, N., A. Schubnel, E. C. David, E. Héripré, Y. Guéguen, and A. Dimanov (2012), Dehydration-induced damage and deformation in gypsum and implications for subduction zone process, *J. Geophys. Res.*, *117*, B03205, doi:10.1029/2011JB008730.

Brown, R., and J. Korringa (1975), On the dependence of the elastic properties of a porous rock on the compressibility of the pore fluid, *Geophysics*, *40*, 608–616, doi:10.1190/1.1440551.

Christensen, N. I. (1984), Pore pressure and oceanic crustal seismic structure, *Geophys. J. R. Astron. Soc.*, *79*, 411–423, doi:10.1111/j.1365-246X.1984.tb02232.x.

David, E. C. (2012), The effect of stress, pore fluid and pore structure on elastic wave velocities in sandstones, PhD dissertation, Imperial Coll. London, London.

Dvorkin, J., G. Mavko, and A. Nur (1995), Squirt flow in fully saturated rocks, *Geophysics*, *60*(1), 97–107, doi:10.1190/1.1443767.

Fortin, J., Y. Guéguen, and A. Schubnel (2007), Effects of pore collapse and grain crushing on ultrasonic velocities and Vp/Vs, *J. Geophys. Res.*, *112*, B08207, doi:10.1029/2005JB004005.

Fortin, J., S. Stanchits, S. Vinciguerra, and Y. Guéguen (2011), Influence of thermal and mechanical cracks on permeability and elastic wave velocities in a basalt from Mt. Etna volcano subjected to elevated pressure, *Tectonophysics*, *503*, 60–74, doi:10.1016/j.tecto.2010.09.028.

Guéguen, Y., and J. Sarout (2009), Crack-induced anisotropy in crustal rocks: Predicted dry and fluid saturated Thomsen's parameters, *Phys. Earth Planet. Inter.*, *172*, 116–124, doi:10.1016/j.pepi.2008.05.020.

Kachanov, M. (1993), Elastic solids with many cracks and related problems, *Adv. Appl. Mech.*, *30*, 259–445, doi:10.1016/S0065-2156(08)70176-5.

Kodaira, S., T. Iidaka, A. Kato, J.-O. Park, T. Iwasaki, and Y. Kaneda (2004), High Pore fluid pressure may cause silent slip in the Nankai Trough, *Science*, *304*, 1295–1298, doi:10.1126/science.1096535.

Le Ravalec, M., and Y. Guéguen (1996), High and low frequency elastic moduli for a saturated porous/cracked rock—Differential self consistent and poroelastic theories, *Geophysics*, *61*, 1080–1094, doi:10.1190/1.1444029.

Mainprice, D., and B. Ildefonse (2009), Seismic anisotropy of subduction zone minerals-contribution of hydrous phases, in *Subduction Zone Geodynamics*, edited by S. Lallemand and F. Funiciello, pp. 63–84, Springer, Berlin, doi:10.1007/978-3-540-87974-9_4.

Mavko, G., T. Mukerji, and J. Dvorkin (1998), *The Rock Physics Handbook*, 273 pp., Cambridge Univ. Press, New York.

Murphy, W. (1985), Sonic and ultrasonic velocities: Theory versus experiment, *Geophys. Res. Lett.*, *12*(2), 85–88, doi:10.1029/GL012i002p00085.

Nishizawa, O. (1982), Seismic velocity anisotropy in a medium containing oriented cracks: Transverse isotropy case, *J. Phys. Earth*, *30*, 331–347, doi:10.4294/jpe1952.30.331.

Nishizawa, O., and K. Kanagawa (2010), Seismic velocity anisotropy of phyllosilicate-rich rocks: Characteristics inferred from experimental and crack-model studies of biotite-rich schist, *Geophys. J. Int.*, *182*, 375–388, doi:10.1111/j.1365-246X.2010.04614.x.

Ougier-Simonin, A., J. Fortin, Y. Guéguen, A. Schubnel, and F. Bouyer (2011), Cracks in glass under triaxial conditions, *Int. J. Eng. Sci.*, *49*, 105–121, doi:10.1016/j.ijengsci.2010.06.026.

Peacock, S. M., N. I. Christensen, M. G. Bostock, and P. Audet (2011), High pore pressures and porosity at 35km depth in the Cascadia subduction zone, *Geology*, *39*(5), 471–474, doi:10.1130/G31649.1.

Popp, T., and H. Kern (1993), Thermal dehydration reactions characterized by combined measurements of electrical conductivity and elastic wave velocities, *Earth Planet. Sci. Lett.*, *120*, 43–57, doi:10.1016/0012-821X(93)90022-2.

Saenger, E. H., O. S. Kruger, and S. A. Shapiro (2004), Effective elastic properties of randomly fractured soils: 3D numerical experiments, *Geophys. Prospect.*, *52*, 183–195, doi:10.1111/j.1365-2478.2004.00407.x.

Sarout, J., and Y. Guéguen (2008), Anisotropy of elastic wave velocities in deformed shales: Part 1—Experimental results, *Geophysics*, *73*(5), D75, doi:10.1190/1.2952744.

Schubnel, A., P. M. Benson, B. D. Thompson, J. F. Hazzard, and R. P. Young (2006), Quantifying damage saturation and anisotropy in cracked rocks by inverting elastic wave velocities, *Pure Appl. Geophys.*, *163*, 947–973, doi:10.1007/s00024-006-0061-y.

Stanchits, S., S. Vinciguerra, and G. Dresen (2006), Ultrasonic velocities, acoustic emission characteristics and crack damage of basalt and granite, *Pure Appl. Geophys.*, *163*, 975–994, doi:10.1007/s00024-006-0059-5.

Thomsen, L. (1986), Weak elastic anisotropy, *Geophysics*, *51*, 1954–1966, doi:10.1190/1.1442051.

Walsh, J. B. (1965), The effect of cracks on the compressibility of rock, *J. Geophys. Res.*, *70*, 381–389, doi:10.1029/JZ070i002p00381.

Winkler, K. (1986), Estimates of velocity dispersion between seismic and ultrasonic frequencies, *Geophysics*, *51*, 183–189, doi:10.1190/1.1442031.